China Ocean Eng., 2019, Vol. 33, No. 6, P. 704–712
DOI: 10.1007/s13344-019-0068-7, ISSN 0890-5487
http://www.chinaoceanengin.cn/ E-mail: coe@nhri.cn

Dynamic Behaviors of A Marine Riser Under Two Different Frequency Parametric Excitations

XIE Wu-de, XU Wan-hai, ZHAI Li-bin, GAO Xi-feng*, XU Zeng-wei

State Key Laboratory of Hydraulic Engineering Simulation and Safety, Tianjin University, Tianjin 30072, China

Received December 7, 2018; revised June 21, 2019; accepted July 24, 2019

Abstract

The marine risers are often subjected to parametric excitations from the fluctuation top tension. The top tension on the riser may fluctuate with multiple frequencies caused by irregular waves. In this paper, the influence between different frequency components in the top tension on the riser system is theoretically simulated and analyzed. With the Euler−Bernoulli beam theory, a dynamic model for the vibrations of the riser is established. The top tension is set as fluctuating with time and it has two different frequencies. The influences from the fluctuation amplitudes, circular frequencies and phase angles of these frequency components on the riser system are analyzed in detail. When these two frequencies are fluctuating in the stable regions, the riser system may become unstable because $\omega_1+\omega_2\approx 2\Omega_n$. The fluctuation amplitudes of these frequencies have little effect on the components of the vibration frequencies of the riser. For different phase angles, the stability and dynamic behaviors of the riser would be different.

Key words: marine risers, parametric excitations, two different frequency components, stability, dynamic behaviors

Citation: Xie, W. D., Xu, W. H., Zhai, L. B., Gao, X. F., Xu, Z. W., 2019. Dynamic behaviors of a marine riser under two different frequency parametric excitations. China Ocean Eng., 33(6): 704–712, doi: 10.1007/s13344-019-0068-7

1 Introduction

Marine risers are widely used in the field of ocean engineering. They are used to transport oil or gas from seabed wells to surface floating platforms or vessels. Under the actions of waves, the upper platform may heave with time (Xu et al., 2008; Xiao and Yang, 2014; Cabrera-Miranda and Paik, 2018). As a result, the top tension on the riser may fluctuate with time. The riser is parametrically excited (Yang et al., 2013; Xiao et al., 2013). When the top tension fluctuates with multiple frequencies, the stability and dynamic behaviors of the riser would become more complicated, which need further investigations (Nayfeh and Mook, 1995; Kuiper et al., 2008).

As a typical parametrically excited system, the marine riser excited by the fluctuation top tension has been extensively studied for several decades with theories and experiments (Nayfeh and Mook, 1995; Kuiper et al., 2008; Yang and Xiao, 2014; Franzini et al., 2015; Lei et al., 2017a). Hsu (1975) analyzed a vertical hanging string parametrically excited by the fluctuation supported end which was moving up-and-down periodically. When the frequency and amplitude of the motion satisfy certain conditions, the string would become unstable due to parametric resonances, which is dangerous. Patel and Park (1995) investigated a tether of a platform subjected to a fluctuation top tension in theory. The fluctuation of the top tension was described with a cosine function of time. After some derivations, a set of Mathieu equations were obtained. Based on these equations, the stability of the tether was analyzed. Chatjigeorgiou and Mavrakos (2002) performed numerical studies to simulate the nonlinear dynamics of risers when the top tension was harmonically fluctuating with time. Kuiper et al. (2008) employed the Floquet theory to determine the stability of the riser that was parametrically excited. In their study, the unstable regions were divided into three categories for different scenarios. Xiao et al. (2013) analyzed the stability of the riser which was subjected to bi-frequency parametric excitation, in which the second frequency was twice of the first frequency. Based on the linear wave theory, Yang et al. (2013) and Xiao and Yang (2014) simulated a marine riser subjected to fluctuation top tension with multiple frequencies. Franzini et al. (2015) carried out a series of experiments to test the vibrations of the riser in parametric resonances. Subsequently, they built a theoretical model to predict the dynamic behaviors of the riser (Franzini and Mazzilli, 2016). Recently, Cabrera-Miranda and Paik (2018) studied the stochastic fluctuation of the top tension and analyzed its influence on the dynamic buckling of the riser. In addition, some other effects on the parametrically excited riser system have also been investigated by many research-

Foundation item: The study was financially supported by the National Natural Science Foundation of China (Grant No. 51679167 and 51979193) .
*Corresponding author. E-mail: gaoxifeng@tju.edu.cn

ers. Lei et al. (2017a) and Meng et al. (2018) took the influence of the internal fluid flow into account and found that the riser system was more unstable with the increase of the internal flow velocity. Lei et al. (2014, 2017b) theoretically studied the riser excited by the fluctuation top tension and the external regular and irregular waves. Moreover, the parametric excitation of the fluctuation top tension combined with vortex-induced vibrations has been investigated by Wang et al. (2015), Zhang and Tang (2015), Yuan et al. (2018) and Zhang et al. (2018).

The floating platform on the sea surface is usually subjected to irregular waves, currents and winds. The platform may heave with multiple frequencies. As a result, the top tension on the riser may fluctuate with multi-frequency. For different combinations of frequencies, the top tension fluctuates differently and the riser is differently excited parametrically. However, the influence between different frequency components on the riser system has not been fully investigated and some aspects are still unknown. Therefore, this paper is aimed to investigate the influence between the frequency components of the top tension on the riser system that is parametrically excited. The stability and dynamic behaviors of the riser are mainly considered. The influences from the fluctuation amplitudes, circular frequencies and phase angles are analyzed in detail.

The rest of this paper is organized as follows. In Section 2, a theoretical model for the vibrations of the riser is established. The top tension is set at fluctuating with time with two different frequency components. The solution methods and the model validation are presented in Section 3. In Section 4, the influences from different aspects of frequency components on the riser system are analyzed. At last in Section 5, the conclusions of this paper are summarized.

2 Theoretical model

As shown in Fig. 1, a common riser system is taken into account. This riser is connected to the seabed and the sea surface floating platform. It is uniform with a total length of L and outer diameter of D. To describe the motion of the riser, a rectangular coordinate system o-yz is established at the bottom end of the riser. The y-axis and z-axis are in the horizontal and vertical directions, respectively.

Because of irregular waves, the top tension on the riser may fluctuate with multi-frequency. To analyze the influence between different frequency components on the riser system, two different frequency components are typically considered. Then the fluctuation top tension is expressed as (Kuiper et al., 2008; Yang et al., 2013; Xiao et al., 2013)

$$N_{\text{top}}(t) = N_0 + k[a_1 \sin(\omega_1 t + \theta_1) + a_2 \sin(\omega_2 t + \theta_2)], \tag{1}$$

where N_0 is the static top tension, k is the stiffness of the tensioner and t is the time. a_1, a_2, ω_1, ω_2, θ_1 and θ_2 are the fluctuation amplitudes, circular frequencies and phase angles of these two frequency components, respectively.

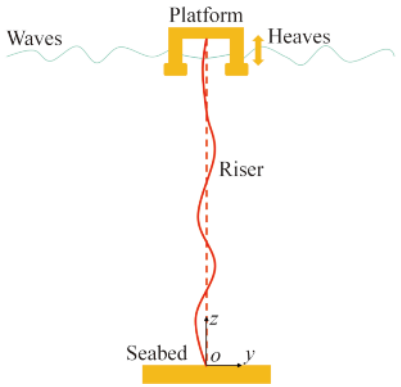

Fig. 1. A marine riser parametrically excited by the fluctuation top tension.

The marine riser is very long and flexible. The shear deformation and rotatory inertia can be neglected. According to the Euler-Bernoulli beam theory, the governing equation for the vibrations of the riser is expressed as (Patel and Park, 1995):

$$EI\frac{\partial^4 y}{\partial z^4} - \frac{\partial}{\partial z}\left[N_{\text{e}}(t)\frac{\partial y}{\partial z}\right] + M\frac{\partial^2 y}{\partial t^2} = f_{\text{d}}, \tag{2}$$

where EI is the bending stiffness and $N_{\text{e}}(t)$ is the effective tension on the riser. M is the total mass of the riser for per unit length, which includes the pipe structural mass, internal fluid mass and external fluid added mass. f_{d} is the external fluid damping. The effective tension on the riser $N_{\text{e}}(t)$ is written as:

$$N_{\text{e}}(t) = N_{\text{top}}(t) - W(z - L), \tag{3}$$

in which W is the submerged weight of the riser for per unit length. According to the studies of Kuiper et al. (2007, 2008), the external fluid damping f_{d} can be expressed as:

$$f_{\text{d}} = -\mu A_1 \frac{\partial y}{\partial t} - \frac{1}{2}\rho_{\text{f}} D A_2 \left|\frac{\partial y}{\partial t}\right| \frac{\partial y}{\partial t}, \tag{4}$$

in which μ is the dynamic viscosity of the external fluid and ρ_{f} is the external fluid density. A_1 and A_2 are two dimensionless constants which can be obtained with experiments. By substituting Eqs. (1), (3) and (4) into Eq. (2), the governing equation of the riser is derived as (Kuiper et al., 2008):

$$EI\frac{\partial^4 y}{\partial z^4} - \frac{\partial}{\partial z}\{[N_0 + ka_1 \sin(\omega_1 t + \theta_1) + ka_2 \sin(\omega_2 t + \theta_2) - W(z - L)]\frac{\partial y}{\partial z}\} + \mu A_1 \frac{\partial y}{\partial t} + \frac{1}{2}\rho_{\text{f}} D A_2 \left|\frac{\partial y}{\partial t}\right| \frac{\partial y}{\partial t} + M\frac{\partial^2 y}{\partial t^2} = 0. \tag{5}$$

Both ends of the riser are simply supported. The boundary conditions are

$$y|_{z=0} = 0,\ \left.\frac{\partial^2 y}{\partial z^2}\right|_{z=0} = 0,\ y|_{z=L} = 0,\ \left.\frac{\partial^2 y}{\partial z^2}\right|_{z=L} = 0. \tag{6}$$

Introduce dimensionless variables and parameters $\eta = y/L$, $\xi = z/L$, $\tau = t\sqrt{EI/(ML^4)}$, $\Pi = N_0 L^2/(EI)$,

$\delta_1 = ka_1L^2/(EI)$, $\delta_2 = ka_2L^2/(EI)$, $\omega_1^* = \omega_1\sqrt{ML^4/(EI)}$, $\omega_2^* = \omega_2\sqrt{ML^4/(EI)}$, $w = WL^3/(EI)$, $\zeta_1 = \mu A_1L^2/\sqrt{EIM}$, $\zeta_2 = A_2\rho_f DL/(2M)$.

The governing equation is expressed in dimensionless form as:

$$\frac{\partial^4\eta}{\partial\xi^4} + w\frac{\partial\eta}{\partial\xi} - \left[\Pi + \delta_1\sin\left(\omega_1^*\tau+\theta_1\right) + \delta_2\sin\left(\omega_2^*\tau+\theta_2\right) - w(\xi-1)\right]\frac{\partial^2\eta}{\partial\xi^2} + \zeta_1\frac{\partial\eta}{\partial\tau} + \zeta_2\left|\frac{\partial\eta}{\partial\tau}\right|\frac{\partial\eta}{\partial\tau} + \frac{\partial^2\eta}{\partial\tau^2} = 0. \tag{7}$$

Similarly, the dimensionless boundary conditions are

$$\eta|_{\xi=0} = 0,\ \left.\frac{\partial^2\eta}{\partial\xi^2}\right|_{\xi=0} = 0,\ \eta|_{\xi=1} = 0,\ \left.\frac{\partial^2\eta}{\partial\xi^2}\right|_{\xi=1} = 0. \tag{8}$$

3 Solution methods and model validation

The dimensionless governing equation (Eq. (7)) is a partial differential equation with respect to the dimensionless axial coordinate ξ and the dimensionless time τ. It can be transformed into a set of ordinary differential equations only related to the time τ by utilizing central difference formulae (Kuiper et al., 2008). The riser is equally divided into n segments and each segment has a dimensionless length of l=1/n. A set of nodes numbered from 0 to n are used to connect these segments. The second-order central difference formulas with respect to ξ are written as:

$$\frac{\partial\eta_i}{\partial\xi} = \frac{\eta_{i+1}-\eta_{i-1}}{2l},\ \frac{\partial^2\eta_i}{\partial\xi^2} = \frac{\eta_{i+1}-2\eta_i+\eta_{i-1}}{l^2},$$
$$\frac{\partial^4\eta_i}{\partial\xi^4} = \frac{\eta_{i+2}-4\eta_{i+1}+6\eta_i-4\eta_{i-1}+\eta_{i-2}}{l^4}, \tag{9}$$

where i (=1, 2, …, n−1) stand for the connected nodes. By substituting Eq. (9) into Eq. (7), the governing equation is expressed as:

$$\frac{\eta_{i+2}-4\eta_{i+1}+6\eta_i-4\eta_{i-1}+\eta_{i-2}}{l^4} + w\frac{\eta_{i+1}-\eta_{i-1}}{2l} - \left[\Pi + \delta_1\sin\left(\omega_1^*\tau+\theta_1\right) + \delta_2\sin\left(\omega_2^*\tau+\theta_2\right) - w(\xi_i-1)\right]\frac{\eta_{i+1}-2\eta_i+\eta_{i-1}}{l^2} + \zeta_1\frac{\partial\eta_i}{\partial\tau} + \zeta_2\left|\frac{\partial\eta_i}{\partial\tau}\right|\frac{\partial\eta_i}{\partial\tau} + \frac{\partial^2\eta_i}{\partial\tau^2} = 0,$$
$$i = 1,2,...,n-1. \tag{10}$$

To deal with the boundary conditions of the riser, two virtual segments with two connected nodes (−1 and n+1) are placed at the first and last of the riser, respectively. The boundary conditions are formulated as:

$$\eta_0 = 0, \eta_{-1} = -\eta_1, \eta_n = 0, \eta_{n+1} = -\eta_{n-1}. \tag{11}$$

The equations in Eq. (10) can be solved with the fourth-order Runge−Kutta method in the time domain (Kuiper et al., 2008). A small perturbation is usually given on the riser as the initial condition. Then the dynamic responses are simulated. The vibration frequencies of the riser are obtained through the Fast Fourier Transform technique with respect to the steady-state responses.

To validate the present model and the solution methods, the experiments performed by Franzini et al. (2015) can be taken for comparison. In the experiments, a model riser was submerged in the fluid and it was excited by a fluctuation top tension. The vibrations of the riser were measured with an optical tracking system. The main physical parameters of the experiment are listed in Table 1. The cases of f_t=2f_N and f_t=3f_N are selected for comparison, where f_t is the fluctuation frequency of the top tension and f_N (=0.84 Hz) is the first mode natural frequency of the riser. In the study of Franzini et al. (2015), the modal responses were calculated with $u_n(t) = \int_0^L y(z,t)\phi_n(z,t)\mathrm{d}z \Big/ \int_0^L \phi_n^2(z,t)\mathrm{d}z$, where $\phi_n(z) = \sin(n\pi z/L)$ is the modal function of the riser.

Table 1 Physical parameters of the experiment (Franzini et al., 2015)

Parameter	Value
Stretched length, L	2.602 m
Outer diameter, D	0.222 m
Mass, m	1.19 kg/m
Axial stiffness, EA	1200 N
Bending stiffness, EI	0.056 Nm^2

In the case f_t=2f_N, Figs. 2a and 2b plot the first modal response and the associated PSD, respectively. It can be seen that the results of the present model and the experiment are in reasonable agreement. For the case of f_t=3f_N, the response of the third mode has the largest amplitudes (Franzini et al., 2015). With the comparison in Figs. 2c and 2d, it can be seen that the results of the present model and the experiment are also in good agreement. Therefore, the present model is reliable to predict the dynamic behaviors of marine risers which are parametrically excited by the fluctuation top tension.

4 Numerical results and analyses

When the top tension on the riser fluctuates with multiple frequencies, the riser system is different for different combinations of frequencies. To investigate the influence between different frequency components on the riser system, a fluctuation top tension with two different frequencies is considered in this paper. The marine riser given by Kuiper et al. (2008) can be taken into account. The main physical parameters are listed in Table 2. The static top tension N_0 is taken as 1.3 times the submerged weight of the riser. The stiffness of the tensioner is k=WL/a_c, where a_c is the critical heave amplitude of the platform (a_c=10 m). Kuiper et al. (2008) analyzed the stability of the parametrically excited riser with a single frequency. Some parametric resonances were determined with the Floquet theory. It was found that for larger external fluid damping or smaller tensioner stiffness, the riser system is more stable. In the present study, the top tension of the riser is firstly fluctuating with a single frequency and then with two different frequencies.

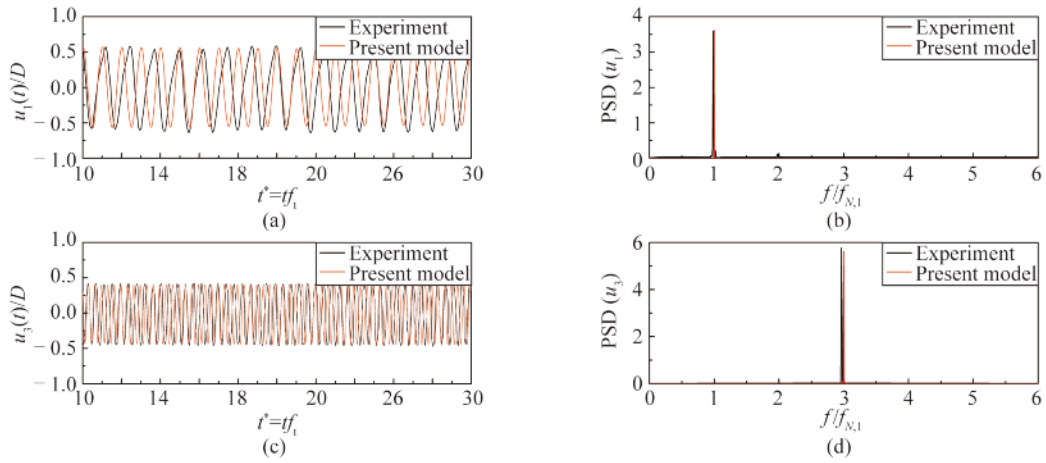

Fig. 2. Comparisons of the present model with the experiment of Franzini et al., (2015) at (a, b) $f_t=2f_N$ and (c, d) $f_t=3f_N$; (a, c) the modal responses and (b, d) the associated PSD.

Table 2 Physical parameters of the riser system (Kuiper et al., 2008)

Parameter	Value
Length, L	2000 m
Outer diameter, D	0.25 m
Inner diameter	0.22 m
Mass, M	136.7 kg/m
Submerged weight, W	735.3 N/m
Elastic modulus, E	2.1×10^{11} N/m^3
Sea water density, ρ_f	1025 kg/m^3
Sea water dynamic viscosity, μ	1.00×10^{-3} kg·s/m

4.1 A single frequency component

When the top tension fluctuates with a single frequency, the stability and dynamic behaviors of the riser can be simulated with the present model. The vibrations of the riser may be different for different fluctuation amplitudes (a_1) and circular frequencies (ω_1). The fluctuation amplitude a_1 is calculated from 1 m to 2 m with an increment of 0.02 m. Meanwhile, the circular frequency ω_1 is increased from 1.2 rad/s to 2.2 rad/s with a step of 0.01 rad/s. The phase angle of the first frequency component θ_1 is set as zero. The influence from the second frequency component is neglected with $a_2=\omega_2=\theta_2=0$. The maximum root-mean-square (rms) displacements of the riser are calculated and plotted in Fig. 3.

In Fig. 3, it can be seen that when the top tension fluctuates with different amplitudes and different circular frequencies, the riser system would be stable or unstable. In the parametric resonances of $\omega_1=2\Omega_5$, $2\Omega_6$, $2\Omega_7$ and $2\Omega_8$ (Kuiper et al., 2008), the riser system is unstable. Out of these resonances, the riser system is stable. In the unstable regions, the maximum rms displacements of the riser are increased with the increase of the fluctuation amplitude a_1. In the stable regions, however, the riser vibration displacements are always very small.

To display the dynamic behaviors of the riser in the unstable regions, the case of $a_1=1.6$ m and $\omega_1=2\Omega_6$ is selected from Fig. 3. The vibration shapes of the riser, the fluctuation of the top tension, the largest displacement and the amplitude spectrum are plotted in Fig. 4.

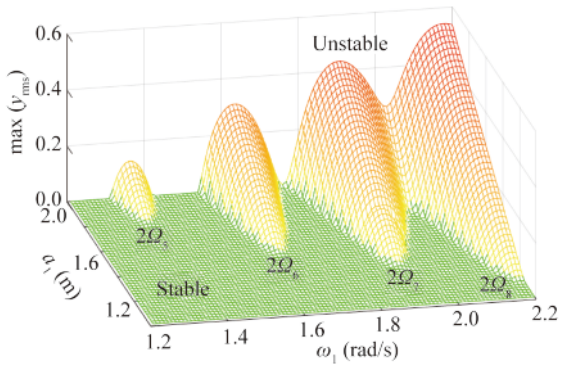

Fig. 3. Maximum rms displacements of the riser under single-frequency parametric excitation.

Fig. 4a clearly shows that the sixth mode of the riser dominates this vibration. The time histories of the top tension and the largest displacement of the riser are plotted in Figs. 4b and 4c, respectively. They are uniform and periodic. In the frequency domain, the vibration of the riser has only one response frequency, as shown in Fig. 4d. This response frequency is half of the frequency of the top tension.

4.2 Two different frequency components

When the top tension fluctuates with two different frequency components, the stability and dynamic behaviors of the riser would be different for different fluctuation amplitudes, circular frequencies and phase angles. These influences on the riser system are analyzed as follows.

4.2.1 *Influence of the fluctuation amplitudes a_1 and a_2*

Firstly, the influence from the fluctuation amplitudes (a_1 and a_2) on the riser system is analyzed. There are three cases for them, i.e., $a_1>a_2$, $a_1=a_2$ and $a_1<a_2$. So the values of them can be taken as $a_1=1.6$ m, $a_2=1.4$ m, 1.6 m and 1.8 m.

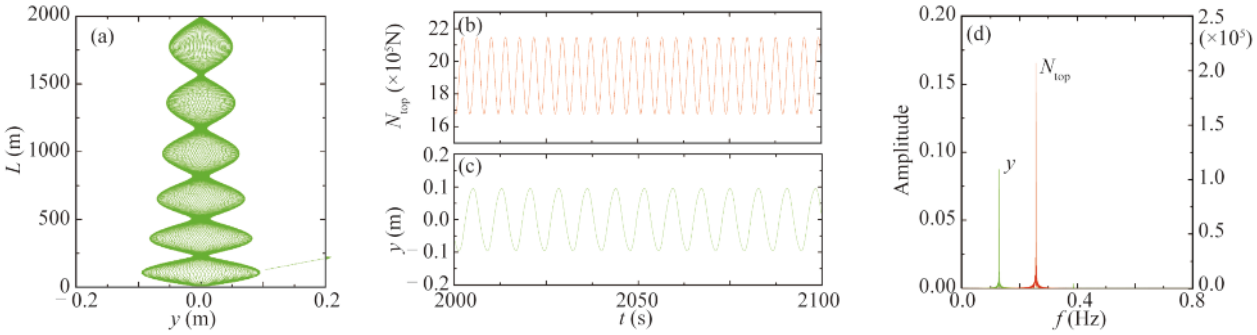

Fig. 4. Dynamic behaviors of the riser at a_1=1.6 m, $\omega_1=2\Omega_6$, θ_1=0 and $a_2=\omega_2=\theta_2$=0: (a) vibration shapes of the riser, (b) time trace of the top tension, (c) the largest displacement, and (d) the amplitude spectra.

The circular frequencies ω_1 and ω_2 are both calculated from 1.2 rad/s to 2.2 rad/s with an increment of 0.01 rad/s. The phase angles θ_1 and θ_2 are both set as zeroes. The maximum rms displacements of the riser are calculated and plotted in Fig. 5.

In the case of $a_1>a_2$, Fig. 5a shows that as the circular frequency ω_1 increases, the parametric resonances of $2\Omega_6$, $2\Omega_7$ and $2\Omega_8$ are excited. While only the parametric resonances of $2\Omega_7$ and $2\Omega_8$ are excited with the increase of ω_2. When $a_1=a_2$, Fig. 5b shows that the parametric resonances of $2\Omega_6$, $2\Omega_7$ and $2\Omega_8$ are both excited by these two frequencies. For the case of $a_1<a_2$, Fig. 5c shows that the parametric resonances of $2\Omega_6$, $2\Omega_7$ and $2\Omega_8$ are excited by the first

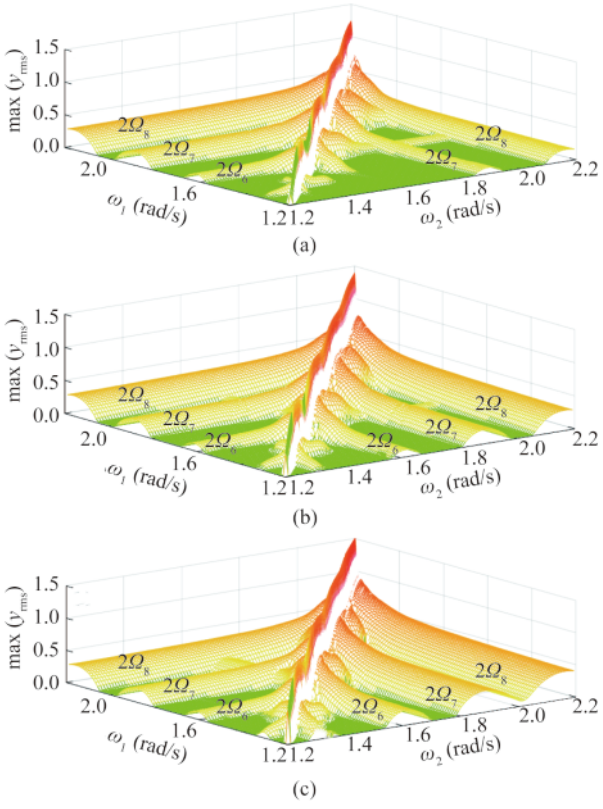

Fig. 5. Maximum rms displacements of the riser under two-frequency parametric excitation for a_1=1.6 m, a_2=1.4 m (a), 1.6 m (b), and 1.8 m (c).

circular frequency ω_1. The second circular frequency ω_2 triggers the parametric resonances of $2\Omega_5$, $2\Omega_6$, $2\Omega_7$ and $2\Omega_8$, which are more. From Fig. 5, it can be known that with the increase of the fluctuation amplitude a_2, the riser system becomes more unstable, and the vibration displacements in the unstable regions increase.

To demonstrate the vibrations of the riser affected by the fluctuation amplitudes, the case of $\omega_1=2\Omega_6$ and $\omega_2=2\Omega_7$ is selected from Fig. 5. In this case, the first circular frequency ω_1 would excite the sixth mode of the riser while the second circular frequency ω_2 would trigger the seventh mode. The riser vibration shapes in Figs. 6a-1, 6a-2 and 6a-3 show that these vibrations are dominated by the seventh mode. The reason for this may be that the riser in the parametric resonance of $\omega_2=2\Omega_7$ could be more affected by the top tension than that in the case of $\omega_1=2\Omega_2$. Fig. 3 could confirm this since the maximum rms displacements of the riser in $2\Omega_7$ are larger than those in $2\Omega_6$.

As the fluctuation amplitude a_2 increases, Figs. 6b-1, 6b-2 and 6b-3 show that the top tension fluctuates with larger amplitudes. As a result, the vibration amplitudes of the riser are increased, as shown in Figs. 6c-1, 6c-2 and 6c-3. However, the time history trends of the top tension and the displacements are almost the same. In the frequency domain (see Figs. 6d-1, 6d-2 and 6d-3), it can be seen that the amplitudes of the response frequencies increase with the increase of the fluctuation amplitude a_2. While the components of the response frequencies seldom change.

4.2.2 *Influence of the circular frequencies ω_1 and ω_2*

The influence of the circular frequencies ω_1 and ω_2 on the riser system should be further analyzed. When $\omega_1=\omega_2$, the displacements of the riser in the diagonal line of Fig. 5 are largely increased. This is because in this condition, these two frequency components in the top tension can be simply added and a single frequency with a large fluctuation amplitude (a_1+a_2) is obtained.

When the circular frequencies ω_1 and ω_2 are both fluctuating in the stable regions, the riser system is usually stable, as shown in Fig. 5. But in some cases, the riser system becomes unstable, especially when ω_1 and ω_2 get close to the

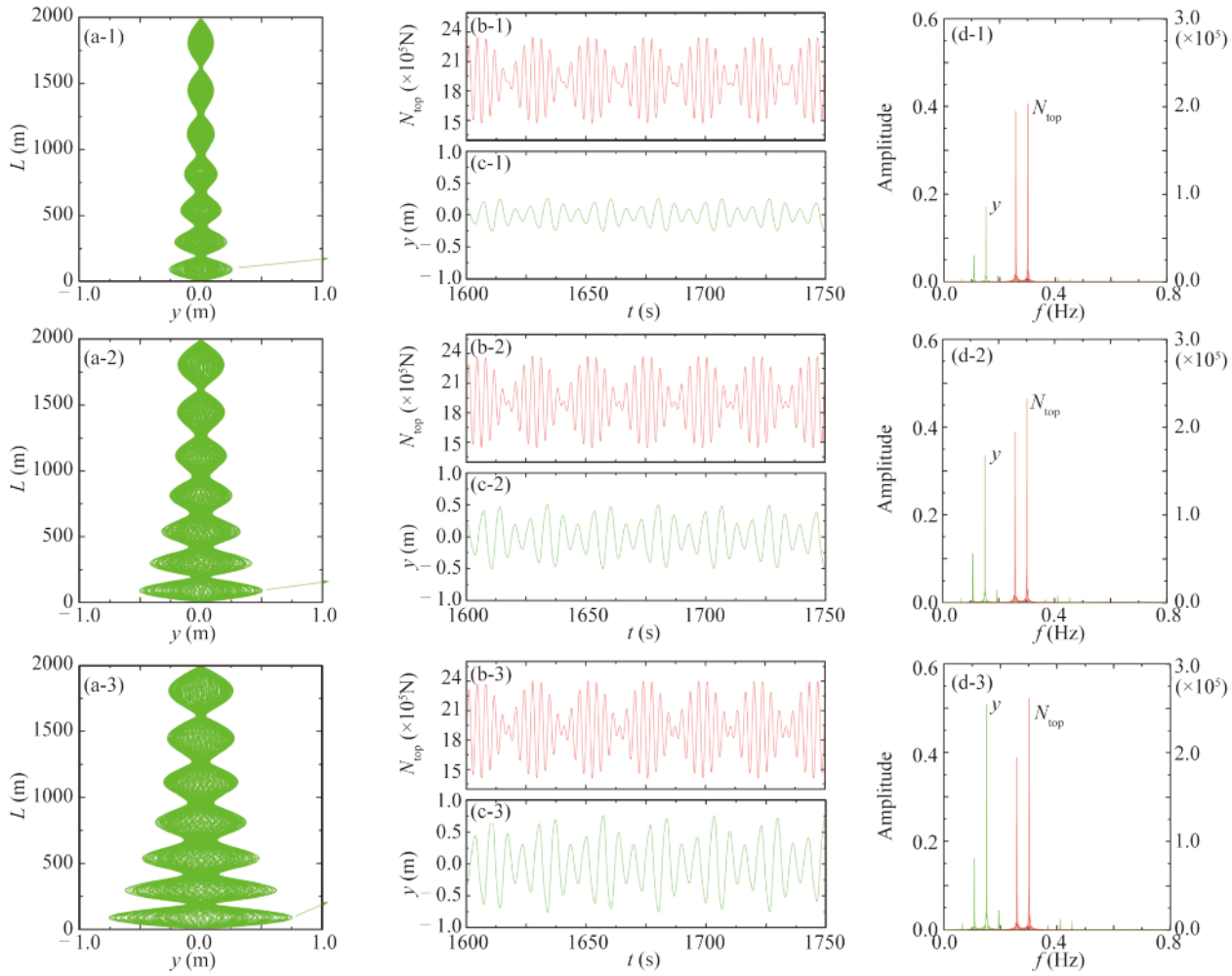

Fig. 6. Dynamic behaviors of the riser at $\omega_1=2\Omega_6$, $\omega_2=2\Omega_7$, and $\theta_1=\theta_2=0$ for a_1=1.6 m, a_2=(−1) 1.4 m, (−2) 1.6 m, and (−3) 1.8 m: (a) vibration shapes of the riser, (b) time trace of the top tension, (c) the largest displacement, and (d) the amplitude spectra.

diagonal line. For instance, the case of ω_1=1.51 rad/s and ω_2=1.59 rad/s is selected from Fig. 5a. The corresponding dynamic behaviors are plotted in Fig. 7. Fig. 7a shows that the riser vibration is dominated by the sixth mode. Figs. 7b and 7c show that the top tension and the vibration displacements of the riser are beating with time. There is a time-lag phenomenon between them. In Fig. 7d, it can be seen that the riser vibration consists of multiple frequencies. These frequencies are smaller than those of the top tension. The reason for the riser system becoming unstable might be that the contributions from ω_1 and ω_2 would excite the parametric resonance of $2\Omega_6$ since $\omega_1+\omega_2\approx2\Omega_6$. In Fig. 5, the parametric resonances of $\omega_1+\omega_2\approx2\Omega_5$ and $\omega_1+\omega_2\approx2\Omega_7$ can also be found.

When one of the circular frequencies is in the stable regions while the other one is in the unstable regions, the riser system is usually unstable, as shown in Fig. 5. To display the dynamic behaviors of the riser, the case of ω_1=1.43 rad/s and $\omega_2=2\Omega_6$ is selected from Fig. 5b. The riser vibration is plotted in Fig. 8. Fig. 8a shows that the sixth mode of the riser dominates this vibration. When comparing Fig. 8a with Fig. 4a, it can be found that the vibration amplitudes of riser are increased. This reflects that the first frequency in the stable regions can still add energy to the riser system. Figs. 8b and 8c illustrate that the top tension and the riser displacement are beating with time. In Fig. 8d, it can be seen that this vibration consists of multiple frequencies.

When these two frequencies are both in the unstable regions, the riser system is unstable, as shown in Fig. 5. For the dynamic responses, the case of $\omega_1=2\Omega_6$ and $\omega_2=2\Omega_6$ is selected from Fig. 5b and plotted in Fig. 9. Fig. 9a shows that the riser vibration is dominated by the sixth mode. When Fig. 9a is compared with Fig. 4a, the increase of the vibration amplitudes can be seen. This is reasonable because the first and second frequencies are both in the parametric resonances and they could both contribute energy to the riser system. In Figs. 9b and 9c, it can be seen that the top tension and the displacement of the riser are beating with time. The riser vibration consists of multi-frequency, as shown in Fig. 9d. The values of them are almost half of those of the top tension.

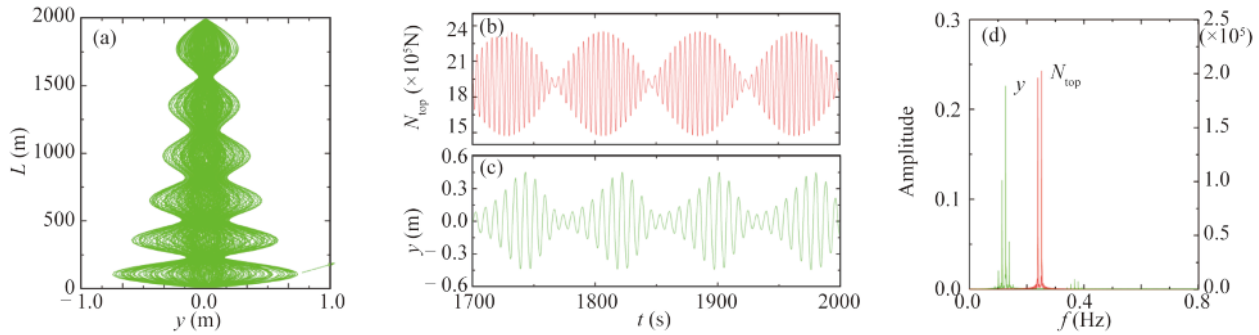

Fig. 7. Dynamic behaviors of the riser at a_1=1.6 m, a_2=1.4 m, ω_1=1.51 rad/s, ω_2=1.59 rad/s, and θ_1=θ_2=0: (a) vibration shapes of the riser, (b) time trace of the top tension, (c) the largest displacement, and (d) the amplitude spectra.

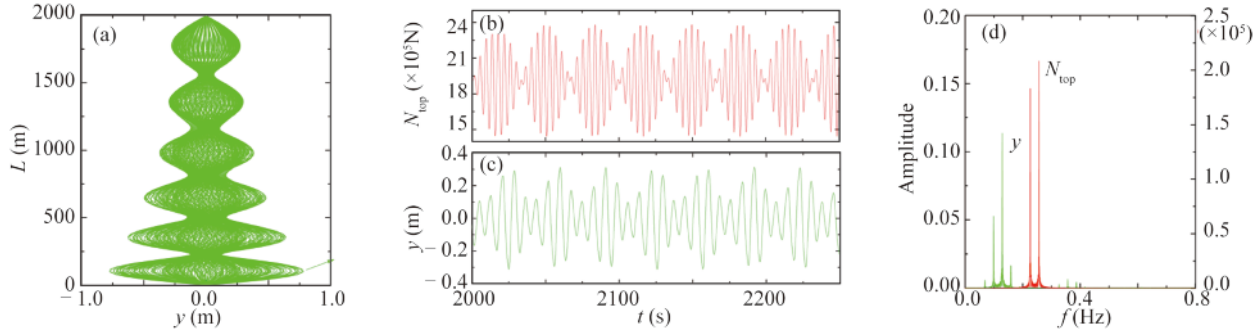

Fig. 8. Dynamic behaviors of the riser at ω_1=1.43 rad/s, ω_2=2Ω_6, a_1=a_2=1.6 m and θ_1=θ_2=0: (a) vibration shapes of the riser, (b) time trace of the top tension, (c) the largest displacement, and (d) the amplitude spectra.

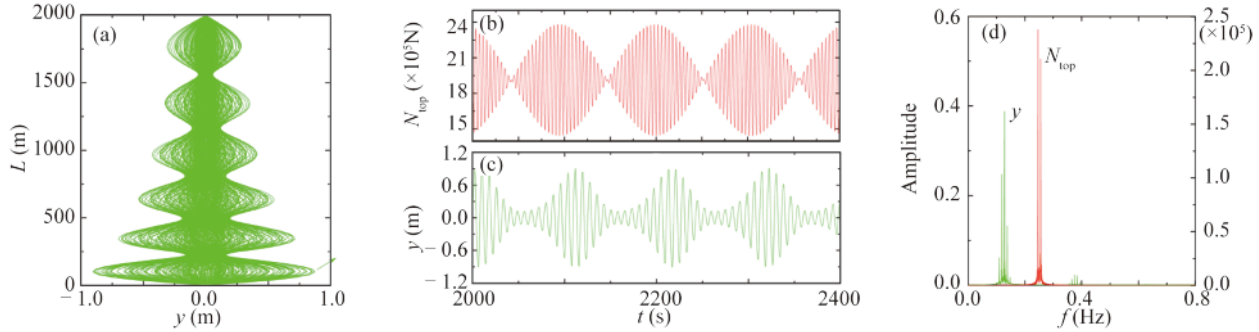

Fig. 9. Dynamic behaviors of the riser at ω_1=2Ω_6, ω_2=2Ω_6, a_1=a_2=1.6 m and θ_1=θ_2=0: (a) vibration shapes of the riser, (b) time trace of the top tension, (c) the largest displacement, and (d) the amplitude spectra.

4.2.3 *Influence of the phase angles θ_1 and θ_2*

The frequency components in the fluctuation top tension may have different phase angles, θ_1 and θ_2, which may cause some effect on the riser system. In order to analyze this effect, the phase angles θ_1 and θ_2 are chosen as random. The circular frequencies of the top tension ω_1 and ω_2 are both calculated from 1.2 rad/s to 2.2 rad/s with an increment of 0.01 rad/s. The fluctuation amplitudes a_1 and a_2 are taken as 1.6 m and 1.4 m, respectively. The maximum rms displacements of the riser are calculated and the results are plotted in Fig. 10.

Compared with Fig. 5a, Fig. 10 shows that as the phase angles θ_1 and θ_2 change randomly, the maximum rms displacements of the riser are different, especially when ω_1 and ω_2 are close to the diagonal line. That means the stability of

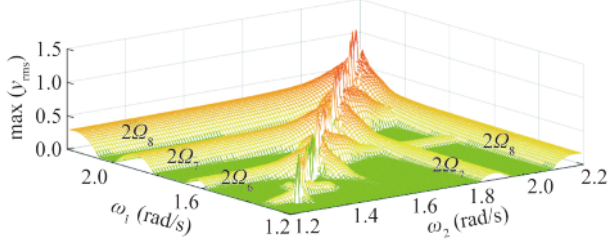

Fig. 10. Maximum rms displacements of the riser under two-frequency parametric excitation for random phase angles θ_1 and θ_2.

the riser system may be different for different phase angles. For the dynamic responses of the riser, the case of $\omega_1=2\Omega_6$ and $\omega_2=2\Omega_7$ can be selected from Fig. 10 and plotted in Fig. 11. Fig. 11a shows that the vibration of the riser is dominated by the seventh mode, which is similar to Fig. 6a-1. For random phase angles θ_1 and θ_2, Figs. 11b and 11c show that the time histories of the top tension and the riser displacement are different from the case of $\theta_1=\theta_2=0$, which are plotted in Figs. 6b-1 and 6c-1. In the frequency domain, Fig. 11d and Fig. 6d-1 show that the components of the vibration frequencies are almost the same. The comparison of Fig. 11 and Fig. 6a shows that the vibrations of the riser in the unstable regions are different for different phase angles.

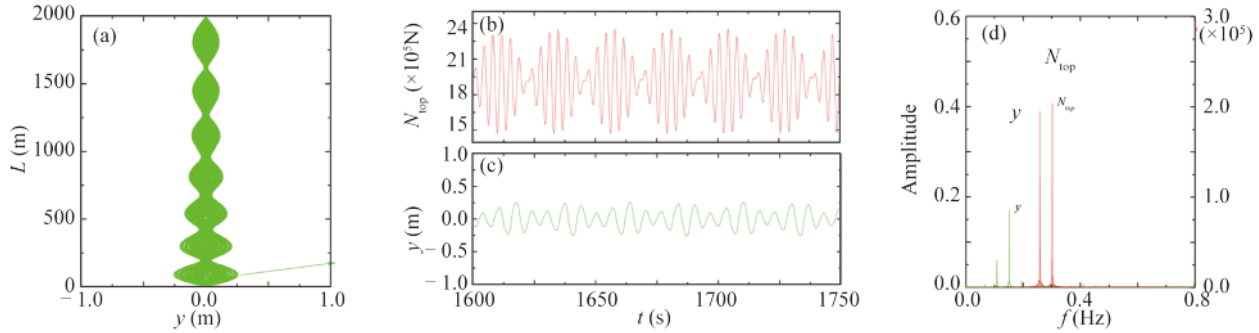

Fig. 11. Dynamic behaviors of the riser at $\omega_1=2\Omega_6$, $\omega_2=2\Omega_7$, $a_1=1.6$ m, $a_2=1.4$ m with random phase angles θ_1 and θ_2: (a) vibration shapes of the riser, (b) time trace of the top tension, (c) the largest displacement, and (d) the amplitude spectra.

5 Conclusions

The marine risers are widely used in ocean engineering. They are often subjected to parametric excitations from the fluctuation top tension caused by waves. Owing to irregular waves, the top tension may fluctuate with multi-frequency. In this paper, the influence between different frequency components in the top tension on the riser system is simulated and analyzed. Based on the Euler-Bernoulli beam theory, the governing equation for the vibrations of the riser is established. The top tension is set as fluctuating with time with two different frequencies. The influences from the fluctuation amplitudes, circular frequencies and phase angles are analyzed in detail. The conclusions of this paper are drawn below.

(1) When the top tension fluctuates with two different frequencies, the stability and dynamic behaviors of the riser system will become more complex. When these two frequencies are both fluctuating in the stable regions, the riser system may become unstable because $\omega_1+\omega_2\approx2\Omega_n$. When one frequency is in the stable regions while the other one is in the unstable regions, the riser system is usually unstable. The frequency in the stable regions can still add energy to the riser system. When these two frequencies are both in the unstable regions, the vibrations of the riser would be dominated by the frequency which has larger effect on the riser system.

(2) With the increase of the fluctuation amplitudes of the top tension, the riser system will become more unstable, the vibration amplitudes of the riser in the unstable regions will increase, while the components of the vibration frequencies seldom change.

(3) The stability and dynamic responses of the riser system are both affected by the phase angles of the frequency components in the top tension. In practical engineering, the influence from the phase angles should be taken into account.

References

Cabrera-Miranda, J.M. and Paik, J.K., 2018. Long-term stochastic heave-induced dynamic buckling of a top-tensioned riser and its influence on the ultimate limit state reliability, *Ocean Engineering*, 149, 156–169.

Chatjigeorgiou, I.K. and Mavrakos, S.A., 2002. Bounded and unbounded coupled transverse response of parametrically excited vertical marine risers and tensioned cable legs for marine applications, *Applied Ocean Research*, 24(6), 341–354.

Franzini, G.R. and Mazzilli, C.E.N., 2016. Non-linear reduced-order model for parametric excitation analysis of an immersed vertical slender rod, *International Journal of Non-Linear Mechanics*, 80, 29–39.

Franzini, G.R., Pesce, C.P., Salles, R., Gonçalves, R.T., Fujarra, A.L.C. and Mendes, P., 2015. Experimental analysis of a vertical and flexible cylinder in water: response to top motion excitation and parametric resonance, *Journal of Vibration and Acoustics*, 137(3), 031010.

Hsu, C.S., 1975. The response of a parametrically excited hanging string in fluid, *Journal of Sound and Vibration*, 39(3), 305–316.

Kuiper, G.L., Brugmans, J. and Metrikine, A.V., 2008. Destabilization of deep-water risers by a heaving platform, *Journal of Sound and Vibration*, 310(3), 541–557.

Kuiper, G.L., Metrikine, A.V. and Battjes, J.A., 2007. A new time-domain drag description and its influence on the dynamic behaviour of a cantilever pipe conveying fluid, *Journal of Fluids and Structures*, 23(3), 429–445.

Lei, S., Zhang, W.S., Lin, J.H., Yue, Q.J., Kennedy, D. and Williams, F.W., 2014. Frequency domain response of a parametrically excited riser under random wave forces, *Journal of Sound and Vibration*, 333(2), 485–498.

Lei, S., Zheng, X.Y., Chen, D.Y. and Yi, L., 2017a. Instability analysis of parametrically excited marine risers by extended precise integration method, *International Journal of Structural Stability and Dynamics*, 17(8), 1750096.

Lei, S., Zheng, X.Y. and Kennedy, D., 2017b. Dynamic response of a deepwater riser subjected to combined axial and transverse excitation by the nonlinear coupled model, *International Journal of Non-Linear Mechanics*, 97, 68–77.

Meng, S., Song, S.D., Che, C.D. and Zhang, W.J., 2018. Internal flow effect on the parametric instability of deepwater drilling risers, *Ocean Engineering*, 149, 305–312.

Nayfeh, A.H. and Mook, D.T., 1995. Nonlinear Oscillations, Wiley-VCH, New York.

Patel, M.H. and Park, H.I., 1995. Combined axial and lateral responses of tensioned buoyant platform tethers, *Engineering Structures*, 17(10), 687–695.

Wang, Y.B., Gao, D.L. and Fang, J., 2015. Coupled dynamic analysis of deepwater drilling riser under combined forcing and parametric excitation, *Journal of Natural Gas Science and Engineering*, 27, 1739–1747.

Xiao, F. and Yang, H.Z., 2014. Probabilistic assessment of parametric instability of a top tensioned riser in irregular waves, *Journal of Marine Science and Technology*, 19(3), 245–256.

Xiao, F., Yang, H.Z., Lu, Q.J. and Zhang, L.B., 2013. Vortex-induced parametric resonance of top tensioned riser based on bi-frequency excitation, *The Ocean Engineering*, 31(2), 28–34. (in Chinese)

Xu, W.H., Zeng, X.H., Wu, Y.X. and Liu, J.Y., 2008. Hill instability analysis of TLP tether subjected to combined platform surge and heave motions, *China Ocean Engineering*, 22(4), 533–546.

Yang, H.Z. and Xiao, F., 2014. Instability analyses of a top-tensioned riser under combined vortex and multi-frequency parametric excitations, *Ocean Engineering*, 81, 12–28.

Yang, H.Z., Xiao, F. and Xu, P.J., 2013. Parametric instability prediction in a top-tensioned riser in irregular waves, *Ocean Engineering*, 70, 39–50.

Yuan, Y.C., Xue, H.X. and Tang, W.Y., 2018. A numerical investigation of vortex-induced vibration response characteristics for long flexible cylinders with time-varying axial tension, *Journal of Fluids and Structures*, 77, 36–57.

Zhang, X.D., Gou, R.Y., Yang, W.W. and Chang, X.P., 2018. Vortex-induced vibration dynamics of a flexible fluid-conveying marine riser subjected to axial harmonic tension, *Journal of the Brazilian Society of Mechanical Sciences and Engineering*, 40(8), 365.

Zhang, J. and Tang, Y.G., 2015. Fatigue analysis of deep-water risers under vortex-induced vibration considering parametric excitations, *Journal of Coastal Research*, 73(S1), 652–659.